sciendo

Polish Journal of Chemical Technology, 23, 2, 81—87, 10.2478/pjct-2021-0021

Commercial Kevlar derived activated carbons for CO_2 and C_2H_4 sorption

M. Kaliszewski, M. Zgrzebnicki, A. Kałamaga, S. Pinjara, R.J. Wróbel*

West Pomeranian University of Technology, Szczecin, Faculty of Chemical Technology and Engineering, Department of Catalytic and Sorbent Materials Engineering, Piastów 42, 71-065 Szczecin, Poland
**Corresponding author: e-mail: rwrobel@zut.edu.pl*

The carbonaceous precursor was obtained via pyrolysis of commercial aramid polymer (Kevlar). Additionally the precursor was activated at 1000°C in CO_2 atmosphere for different times. Obtained materials were characterised by BET; XPS; SEM and optical microscopy. The sorption capacities were determined by temperature swing adsorption performed in TGA apparatus for CO_2 and C_2H_4 gases. The obtained materials exhibit high difference in sorption of these gases i.e. 1.5 and 2.8 mmol/g @30°C respectively and high SSA ~1600 m^2/g what can be applied in separation applications. The highest uptakes were 1.8 and 3.1 mmol/g @30°C respectively. It was found that the presence of oxygen and nitrogen functional groups enhances C_2H_4/CO_2 uptake ratio.

Keywords: activated carbon, carbonaceous catalysts, autoxidation, alpha-pinene, iron particles, biomass.

INTRODUCTION

Greenhouse gases accumulate in the atmosphere and create the heat-reflective layer that keeps the Earth temperature friendly for life. It is widely acknowledged that climate change is caused by an excess of anthropogenic greenhouse gases. Some of the most common and worrisome greenhouse gases are CO_2 and CH_4. Carbon dioxide is emitted whenever carbon-rich fossil fuels are burned. Although CO_2 is not the most potent anthropogenic greenhouse gas, it has the largest contribution to climate change due to its volume emitted mostly in the energy sector. On the other hand, anthropogenic methane is emitted in the process of decomposition of organic matter. It is also released from landfills, swamps, cattle farms, rice paddies, etc. CH_4 emissions are lower than CO_2 emissions but it is considered a major greenhouse gas because each methane molecule has 25 times the global warming potential of a carbon dioxide molecule.

To actively address these emerging challenges, capturing the greenhouse gases from the emission sources and utilizing them is considered a direct and highly effective strategy. Carbon dioxide is a very important multipurpose chemical and can be utilized as a freezing medium, foaming agent, green solvent and promising feedstock for the future production of key chemicals[1, 2, 3]. Before CO_2 utilization it has to be separated and recovered from the mixture of gasses, usually from the post-combustion mixture.

The liquid amine-based CO_2 separation commercialized for a very long time still suffers from high energy consumption in the recycling of amine, as well as the amines' toxic, corrosive, and volatile properties. The CO_2 can be also separated by the application of membranes, but the problem can be low durability of membranes at elevated temperatures of flue gases. However, the combination of photocatalysis and membrane separation in the application for CO_2-derived products could alleviate the problem of CO_2 storage after separation[4].

By contrast, solid sorbents that capture CO_2 via physical interactions are more appealing, since the whole process is energy-saving, eco-friendly, and easily reversible[5]. The solid adsorbents have been suggested as alternative candidates for CO_2 separation. Considerable efforts have been devoted to screening suitable CO_2 adsorbents for post-combustion capture application[6–23].

Methane is the valuable chemical stock in chemical industries but the first stage of methane transformation – syngas production is very energy consumed[24]. Despite being the most abundant and least expensive hydrocarbon feed stock available, methane finds limited use as a starting material within the chemical industry[25]. That's why the production of key chemicals and fuels considering the rapid advances in methane direct conversion technologies is very promising. Methane can be utilized as feedstock for methanol[26–28], formaldehyde[29–31], methyl bisulphate[25, 32–35], carbon nanotubes combined with hydrogen[36–40] one-step production excluding the synthesis gas production stage. Methane can be also applied as alternative transportation in compressed natural gas and adsorbed natural gas technology[41].

Although ethylene is not considered a potent global warming agent its removal via sorption is of importance due to its impact on fruit and vegetable ripening. Ethylene is the hormone for plants and its concentration control in the greenhouse atmosphere or during fruits transport can improve growth efficiency and food preservation respectively[42].

Carbonaceous materials, especially activated carbons, are considered attractive materials for gas storage[41–45], adsorption[12, 17–19, 21, 22, 46], energy storage[17, 47–50], and catalysis[51–57] owing to their adsorptive nature. Porous activated carbons[58] can be produced from biomass[13, 15, 17, 21, 59] and commercial activated carbons modification[8, 9, 14, 16, 19], various chemicals[10, 22, 23].

Among the variety of precursors from which carbonaceous materials may be derived the polymers are especially attractive. One of the advantages is the formation of the final shape during polymerization stage. The other advantage is exact and the same characteristic for every batch of produced material. The polymer precursors usually exhibit very high purity. The disadvantage may be the higher price.

An interesting precursor is aramid polymer also known as a Kevlar ®. Kevlar is a kind of polyaramid fibers which was firstly commercialized in 1972 by DuPont. This material has good properties like high-temperature decomposition, flame resistance, abrasion and stretching resistance,

chemically stability, etc[60–62]. It has stab resistance and ballistic property which allows to produce flexible body armours with light weight and high-temperature resistance capacity enables to produce personal protective clothing for the firefighters such as gloves, suits and jackets, breeches. Moreover, plastrons are made for sportswear in motorcycling and car racing[63–66]. The good elongation capacity, abrasion resistance, strength, thermal stability and adaptable weariness resistant, make Kevlar good material to manufacture tires, braking lines and automobile brakes. Many useful carbonaceous materials are derived from Kevlar with great benefits of desired properties, such as Activated Carbon Fibers (ACFs) show fibrous morphology. It improves adsorption rate of the ACFs which is used for effective gas storage. High adsorption capacity is possible to achieve by robust structure, tunable porosity, lightweight, high thermal/chemical stability of Kevlar[67–68]. Aramid Nanofiber (ANF) is made from Kevlar to make composite materials with good cation selectivity and high mechanical strength and are used in nanofluidic osmotic power generators[69]. Polyaramid fibers are used as precursors for microporous carbonaceous materials for gases (e.g. CO_2, N_2, CH_4, O_2) and vapours (e.g. CH_2Cl_2, C_6H_6, C_6H_{12}) adsorption[70–75].

The aramid polymer contains oxygen and nitrogen in its structure. Therefore the Kevlar-derived carbonaceous materials are doped with these elements. The goals of this work were: checking how the time of physical activation influence C_2H_4 and CO_2 uptakes; Determining how the elemental content is changing during activation; Determining the influence of nitrogen and oxygen on sorption properties.

EXPERIMENTAL

The commercial Kevlar fabric was used as a carbonaceous precursor. The Carburisation process was conducted under nitrogen atmosphere at 700°C for 2 hours (ramp 10°C/min). The material obtained in this way will be referred as Carb. The physical activation was conducted under CO_2 atmosphere at 1000°C (ramp 5°C/min). After reaching 1000°C the sample was kept for a given time. The activated carbons will be referred as AC0; AC5; AC15 and AC30 for times of activation ranging from 0 to 30 minutes – e.g. AC15 denotes sample activated 15 minutes at 1000°C.

The textural characterization of the carbonaceous materials was carried out by N_2 adsorption-desorption isotherm measurements at 77 K (Quantachrome; Autosorb Instrument). The samples were degassed at 373 K under vacuum for 16 h prior to analysis. The specific surface areas (SSA) were calculated using the Brunauer–Emmett–Teller (BET) equation. The total pore volumes were evaluated based on the volume adsorbed at a relative pressure of about 0.99. Pore size distribution, as well as the volume of micro- (V_{micro}) and mesopores (V_{meso}), were calculated using QSDFT method.

The sub-micropores of diameters below 1.2 nm volumes were calculated by using the Density Functional Theory (DFT) to the CO_2 adsorption isotherms at 0°C. The software being the part of volumetric apparatus (QuadraWin; Quantachrome Instruments) was used to evaluate the data. The cumulative pore volumes $V_{0.7}$, $V_{0.8}$ and $V_{1.0}$ of pores up to 0.7, 0.8 and 1.0 nm were determined respectively. Also, the specific surface area (S_{CO_2}) of pores up to 0.9 nm was determined.

The X-ray photoelectron spectroscopy measurements were performed in a commercial UHV surface analysis system (PREVAC), which operates at a base pressure in the low 10^{-10} mbar range. The setup is equipped with non-monochromatic X-ray photoelectron spectroscopy (XPS) and kinetic electron energy analyzer (SES 2002; Scienta). The calibration of the spectrometer was performed using Ag $3d_{5/2}$ transition. Samples in the form of fine powder were thoroughly degassed prior to measurement so that during XPS measurements the vacuum was in the low 10^{-9} mbar range. The X-ray photoelectron spectroscopy was performed using Al K_α ($h\nu$ = 1486.6 eV) radiation.

Scanning electron microscopy with cold emission (SU8020; Hitachi) was used to characterize the morphology of the samples. The accelerating voltage was 5 kV. Also, an optical microscope (Stemi 508; Zeiss) was used for characterization in the visible light spectrum.

RESULTS AND DISCUSSION

In Fig 1. There are presented images obtained in optical microscope of Kevlar prior and after pyrolysis/carburization. It can be noticed that net-like structure is preserved after thermal treatment. This feature is an advantage for gas adsorption applications.

In Fig 2. There are presented images obtained via scanning electron microscopy.

The activated material also preserves net-like structure but the individual threads shrink during the process. Closer inspection also reveals the formation of sponge-like structure in the case of activated material. The size of most of the visible pores is about 50 nm. These pores are pathways for the diffusion of gases into much smaller pores below 1 nm size.

The porous morphology was determined from nitrogen adsorption/desorption isotherms presented in Fig. 3. The evaluation of these isotherms enabled the determination

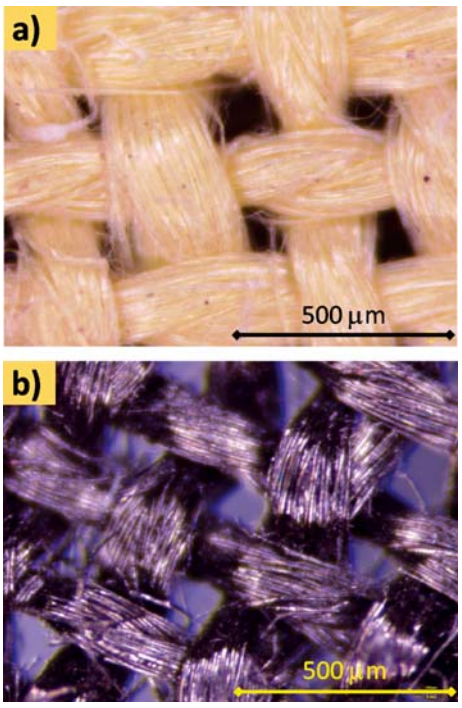

Figure 1. Optical microscopy images: a) Kevlar, b) Carb

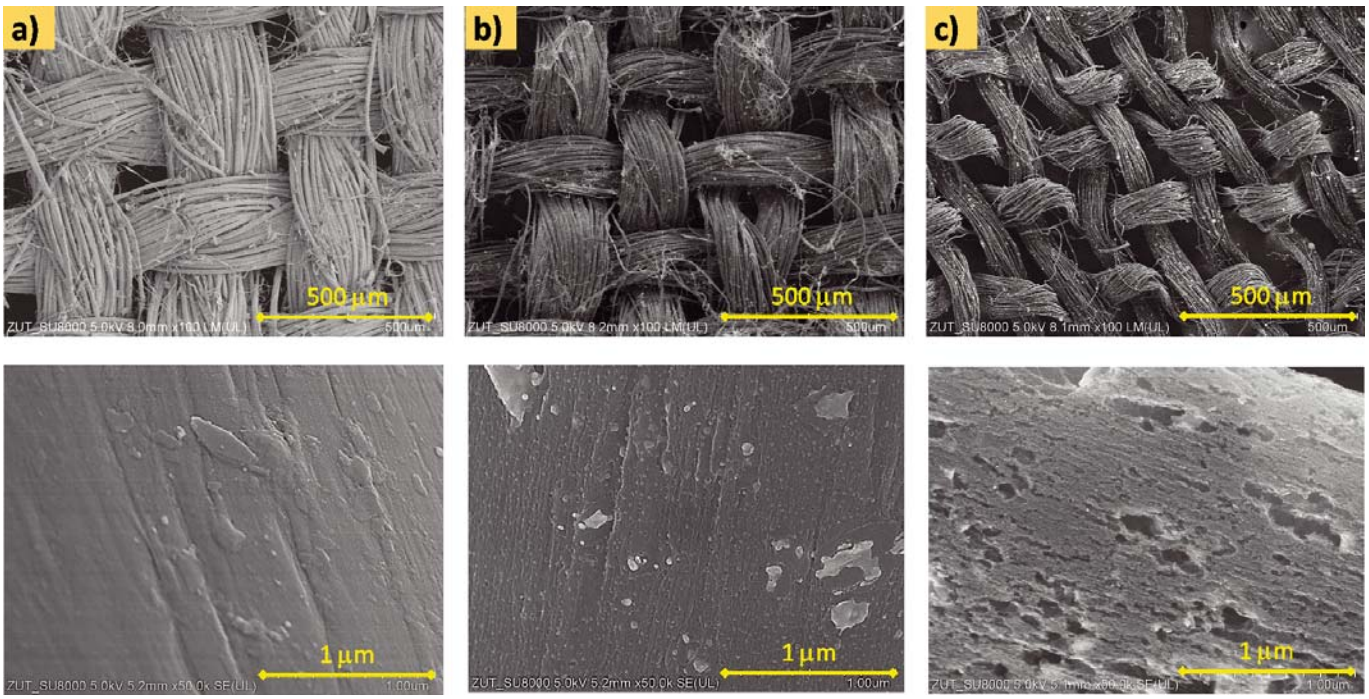

Figure 2. SEM images: a) Kevlar, b) Carb, c) AC30

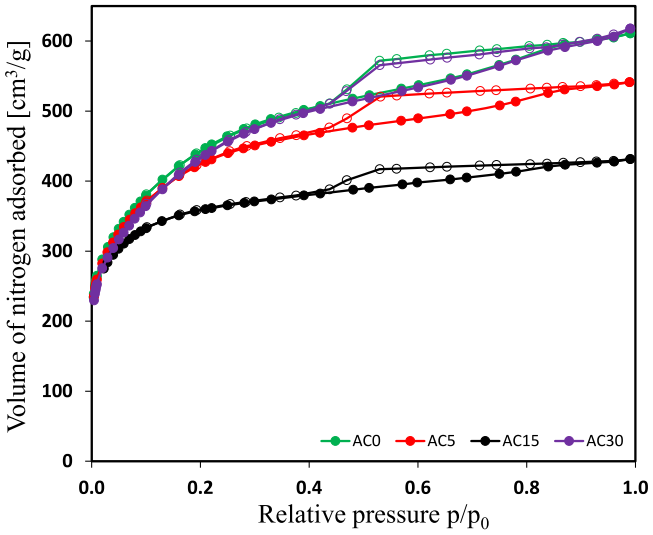

Figure 3. N_2 adsorption/desorption isotherms at 77 K

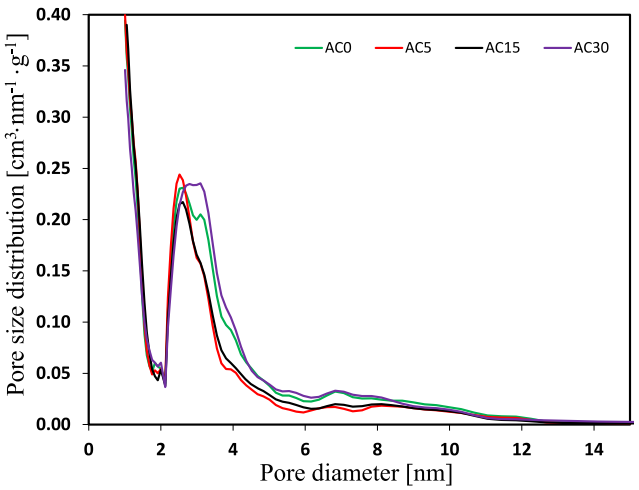

Figure 4. Pore size distributions calculated from N_2 adsorption/desorption isotherms at 77 K

of SSA and pore volumes presented in Table 1. Moreover, the pore size distributions were determined and are presented in Fig. 4.

According to IUPAC, isotherms presented in Figure 3 indicate a combined type of I_b and IVa. Type Ib is characteristic for materials with a broad range of micropores and narrow mesopores up to a diameter of 2.5 nm. Moreover, the microporous structure is confirmed by steep uptake of nitrogen at very low p/p_0 range. On the other hand, type IVa is characteristic for materials with mesoporous structure, which is confirmed by the hysteresis phenomenon occurring for pores wider than 4 nm in diameter.

The analysis of the data presented in Table 1 reveals activation process strongly develops SSA from 3 m^2/g for not activated material (Carb) to about 1600 m^2/g for all activated samples. The total pore volume is negligible for Carb and increases 84–96 times for other samples depending on activation time. Interestingly the Carb sample despite its negligible SSA and total pore volume exhibits significant CO_2 and C_2H_4 uptakes. One should note that for uptakes of these gases are responsible pores below 1.0 nm. The nitrogen sorption method enables pore volume determination in the range 1.2–100.0 nm. Therefore it is expected that Carb sample exhibit a considerable volume of pores below 1.2 nm.

Table 1. Textural parameters of carbonaceous materials and sorption uptakes

Sample	SSA [m^2/g]	Pore volume [cm^3/g]			Uptakes [mmol/g]	
		V_{total}	V_{micro}	V_{meso}	CO_2 at 30°C	C_2H_4 at 30°C
Carb	3	0.01	-	-	1.4	1.4
AC0	1611	0.95	0.35	0.53	1.8	2.8
AC5	1556	0.84	0.37	0.41	1.6	2.5
AC15	1593	0.87	0.39	0.42	1.5	2.8
AC30	1586	0.96	0.32	0.57	1.7	3.1

The CO_2 sorptions at 0°C enabled the determination of pore volumes below 1.2 nm, the specific surface area of such pores and CO_2 uptake at this temperature (Table 2).

The notation $V_{0.7}$, $V_{0.8}$ and $V_{1.0}$ denotes cumulative pore volume of pores up to 0.7, 0.8 and 1.0 nm respectively. Pores 0.7 and 0.8 are crucial for sorption of CO_2 in temperatures 0°C and 30°C respectively. The pores 1.0 nm are crucial for sorption ethylene at 30°C.

The pore size distributions presented in Fig. 4. exhibit considerable amount of micropores in the range 1.2–2.0 nm and mesopores in the range 2.0–12.0 nm. The Carb material is not presented in the figure due to the negligible nitrogen sorption. The highly porous structure is a result of CO_2 activation process. Even sample AC0 underwent activation process by heating up to 1000°C followed by immediate cooling down in CO_2 atmosphere. The main difference one can observe in volume of mesopores which are irrelevant for the sorption of small molecules like CO_2 and C_2H_4 but may be crucial for the sorption of larger molecules like benzene.

The sorption properties are also dependent on the surface chemistry of the sorbents. In Fig. 5 there are presented XPS spectra of all samples with denoted signals.

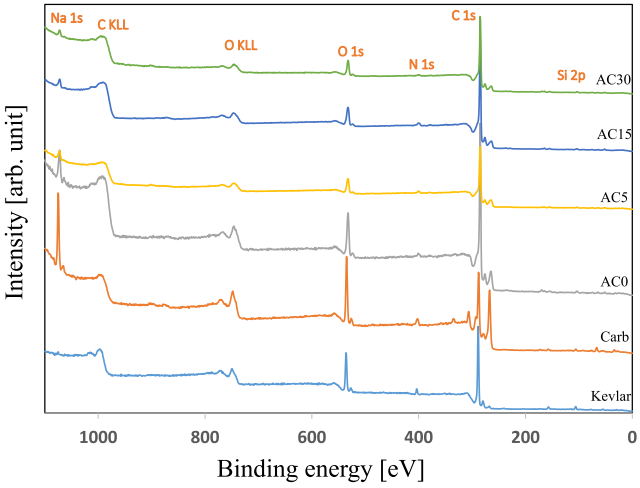

Figure 5. XPS spectra of investigated samples

The Kevlar polymer consists of hydrogen, carbon, nitrogen and oxygen elements. Hydrogen is not detectable with XPS method. Surprisingly the presence of sodium and silicon was found in the samples. The quantitative analysis enabled the determination of elemental surface concentrations presented in Table 3.

The sodium and silicon may be result of commercial-grade material. The silicon element may be antifriction agent during manufacture of Kevlar threads. Therefore it is expected that silicon will be present mainly over the surface of threads. This confirms the high concentration of this element for fabric of Kevlar while pulverised material after carbonisation exhibit lower content of this element. Conversely, sodium exhibits the lowest values for Kevlar fabric indicating that this element is embedded in polymer. Carbonisation of Kevlar at 700°C leads to the highest sodium surface concentration. Activation at 1000°C depletes sodium concentration. This tendency can be explained as follows: the sodium atoms embedded in the polymer diffuse to the surface in the carbonisation process. However, at higher temperatures volatile sodium compounds evaporate and thus lower concentrations are observed. The sodium presence in the polymer may be result of its production procedure. The polymer is produced in strong acid and finally, it requires neutralisation e.g. with sodium base.

Table 3. Elemental surface concentrations as determined by XPS

Sample	Surface concentrations [at.%]				
	C	O	N	Si	Na
Kevlar	78.6	15.0	3.0	3.1	0.3
Carb	66.4	19.6	4.8	1.6	7.6
AC0	84.1	10.6	1.7	1.2	2.4
AC5	82.1	12.0	2.4	1.6	1.9
AC15	89.2	6.9	2.6	0.7	0.6
AC30	87.9	8.4	1.4	1.3	1.0

It was also found that the nitrogen content in Kevlar polymer is lower than expected. The atomic ratio of Carbon/Oxygen/Nitrogen is expected to be 78/11/11. The XPS measured ratio is 81.2/15.5/3.3 respectively. The discrepancy may be result of surface oxidation of polymer and the presence of sodium and silicon oxides.

The analysis of Table 3 shows that oxygen and nitrogen contents decrease with activation time. This may indicate that heteroatoms may be considered as a defect over the carbon surface which facilitates the reaction of CO_2 with carbon.

In Fig. 6 there are presented CO_2 isobars obtained through heating and monitoring the mass of the sample in 250°C and cooling down to 30°C under CO_2 atmosphere. Due to that measurement procedure, the highest desorption occurs at 250°C and is considered as a reference point with 0.0 mmol/g uptake.

Such presentation of the results enables the determination of gas uptakes not only for a single temperature but for the whole 30–250°C range. The sample with the highest CO_2 uptake is AC0. Interestingly the sample without activation process i.e. Carb exhibits comparable CO_2 uptakes above 50°C.

In Fig. 7 there are presented C_2H_4 isobars obtained in the same manner as in case of CO_2.

One can observe that activation leads to significant improvement of C_2H_4 uptakes. The highest performance exhibit the sample AC30 with the longest time of activation.

In Fig. 8. there is a presented graph showing C_2H_4 / CO_2 ratios for all samples.

One can notice that activation increases the preference for C_2H_4 sorption. This feature can be utilised for the separation of these gases. The increase of the ratio

Table 2. Textural parameters of carbonaceous materials and sorption uptakes

Sample	S_{CO2} [m²/g]	Pore volume [cm³/g]			Uptakes [mmol/g]
		$V_{0.7}$	$V_{0.8}$	$V_{1.0}$	CO_2 at 0°C
AC0	679	0.15	0.18	0.21	3.6
AC5	707	0.15	0.18	0.21	3.5
AC15	729	0.17	0.19	0.22	3.8
AC30	670	0.14	0.17	0.20	3.3

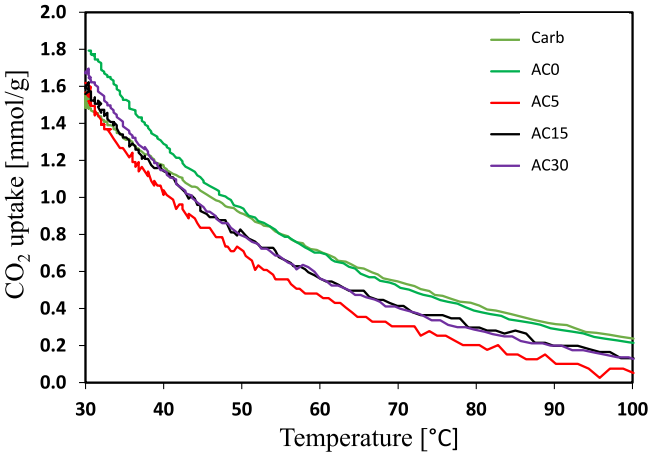

Figure 6. CO_2 isobar at 1 bar

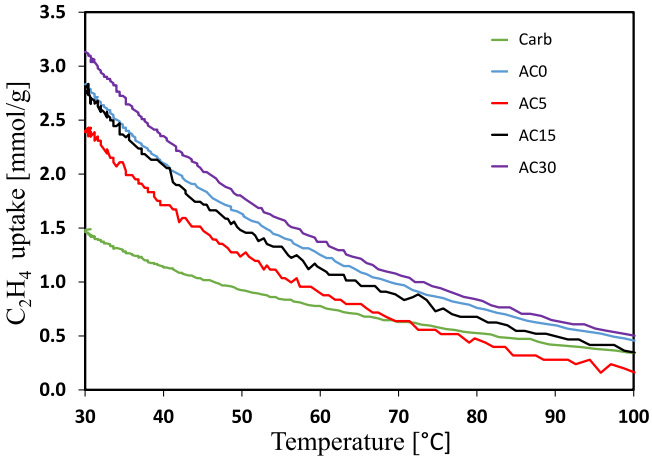

Figure 7. C_2H_4 isobar at 1 bar

correlates well with the decrease of oxygen and nitrogen (c.f. Tab. 2).

SUMMARY AND CONCLUSIONS

Carbon materials derived from commercial Kevlar fabric retain their netlike structure after physical activation. This feature is beneficial for the reduction of flow resistance in the sorption/desorption of liquids and gases.

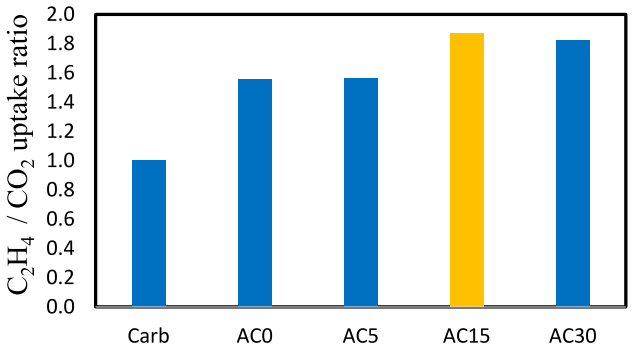

Figure 8. C_2H_4 to CO_2 uptake ratio at 30^{O}C and 1 bar

These materials contain high nitrogen concentrations i.e. 4.8 and 2.6 at. % for not activated and activated material respectively. The commercial-grade Kevlar contains silicon and sodium additives. The highest obtained uptakes at 30°C were 3.1 and 1.8 mmol/g for C_2H_4 and CO_2 respectively. It was observed that the lower content of oxygen and nitrogen in activated carbon the higher C_2H_4/CO_2 ratio. Therefore activated carbons for the separation of these gases should contain low content of heteroatoms.

ACKNOWLEDGMENTS

This research was supported by ZUT Highfliers School (Szkoła Orłów ZUT) project, co-ordinated by Dr. Piotr Sulikowski, within the framework of the program of the Minister of Education and Science (Grant No. MNiSW/2019/391/DIR/KH, POWR.03.01.00-00-P015/18), co-financed by European Social Fund, the amount of financing PLN 1,704,201,66.

LITERATURE CITED

1. Michalkiewicz, B., Majewska, J., Kądziołka, G., Bubacz, K., Mozia, S. & Morawski, A.W. (2014). Reduction of CO_2 by adsorption and reaction on surface of TiO_2-nitrogen modified photocatalyst. *J. CO_2 Util.* 5, 47–52. DOI: 10.1016/j.jcou.2013.12.004.

2. Francke, R., Schille, B. & Roemelt, M. (2018). Homogeneously catalyzed electroreduction of carbon dioxide-methods, mechanisms, and catalysts. Chem. Rev. 118 4631–4701.

3. Xie, C., Chen, C., Yu, Y., Su, J., Li, Y., Somorjai, G.A. & Yang, P. (2017). Tandem catalysis for CO_2 hydrogenation to C_2–C_4 hydrocarbons. *Nano Lett.* 17, 3798–3802.

4. Mozia, S., Darowna, D., Wróbel, R. & Morawski, A.W (2015). A study on the stability of polyethersulfone ultrafiltration membranes in a photocatalytic reactor. *J. Membr. Sci.* 495 176–186. DOI: 10.1016/j.memsci.2015.08.024.

5. Bui, M., Adjiman, C.S., Bardow, A., Anthony, E.J., Boston, A., Brown, S., Fennell, P.S., Fuss, S., Galindo, A. & Hackett, L.A. (2018). Carbon capture and storage. (CCS): the way forward. *Energy Environ. Sci.* 11, 1062–1176.

6. Kapica-Kozar, J., Pirog, E., Wróbel, R.J., Mozia, S., Kusiak-Nejman, E., Morawski, A.W., Narkiewicz, U. & Michalkiewicz, B. (2016). TiO2/titanate composite nanorod obtained from various alkali solutions as CO_2 sorbents from exhaust gases. *Microporous Mesoporous Mater.* 231, 117–127. DOI: 10.1016/j.micromeso.2016.05.024.

7. Lendzion-Bielun, Z., Czekajlo, L., Sibera, D., Moszynski, D., Sreńscek-Nazzal, J., Morawski, A.W., Wróbel, R.J., Michalkiewicz, B., Arabczyk, W. & Narkiewicz, U. (2018). Surface characteristics of KOH-treated commercial carbons applied for CO_2 adsorption. *Adsorp. Sci. Technol.* 36, 478–492. DOI: 10.1177/0263617417704527.

8. Glonek, K., Sreńscek-Nazzal, J., Narkiewicz, U., Morawski, A.W., Wróbel, R.J. & Michalkiewicz, B. (2016). Preparation of Activated Carbon from Beet Molasses and TiO_2 as the Adsorption of CO_2. *Acta Phys. Pol. A* 129, 158–161. DOI: 10.12693/APhysPolA.129.158.

9. Sibera, D., Narkiewicz, U., Kapica, J., Serafin, J., Michalkiewicz, B., Wróbel, R.J. & Morawski, A.W. (2019). Preparation and characterisation of carbon spheres for carbon dioxide capture. *J. Porous Mater.* 26, 19–27. DOI: 10.1007/s10934-018-0601-8.

10. Kapica-Kozar, J., Michalkiewicz, B., Wróbel, R.J., Mozia, S., Pirog, E., Kusiak-Nejman, E., Serafin, J., Morawski, A.W. & Narkiewicz, U. (2017). Adsorption of carbon dioxide on TEPA-modified TiO2/titanate composite nanorods. *New. J. Chem.* 41, 7870–7885. DOI: 10.1039/c7nj01549f.

11. Zgrzebnicki, M., Krauze, N., Gęsikiewicz-Puchalska, A., Kapica-Kozar, J., Pirog, E., Jedrzejewska, A., Michalkiewicz, B., Narkiewicz, U., Morawski, A.W. & Wróbel, R.J. (2017). Impact on CO2 Uptake of MWCNT after Acid Treatment Study. *J. Nanomater.* 2017. DOI: 10.1155/2017/7359591.

12. Serafin, J., Narkiewicz, U., Morawski, A.W., Wróbel, R.J. & Michalkiewicz, B. (2017). Highly microporous activated carbons

from biomass for CO_2 capture and effective micropores at different conditions. *J. CO_2 Util.* 18, 73–79. DOI: 10.1016/j.jcou.2017.01.006.

13. Sreńscek-Nazzal, J. & Kielbasa, K . (2019). Advances in modification of commercial activated carbon for enhancement of CO_2 capture. *Appl. Surf. Sci.* 494, 37–151. DOI: 10.1016/j.apsusc.2019.07.108.

14. Sreńscek-Nazzal, J. & Kielbasa, K . (2020). Microporous carbon foams for CO_2 adsorption obtained from carbon nanospheres. *Przem. Chem.* 99(1), 70–73. DOI: 10.15199/62.2020.1.7.

15. Sreńscek-Nazzal, J., Narkiewicz, U., Morawski, A.W., Wróbel, R.J. & Michalkiewicz, B. (2015). Comparison of Optimized Isotherm Models and Error Functions for Carbon Dioxide Adsorption on Activated Carbon. *J. Chem. Eng. Data* 60, 3148–3158. DOI: 10.1021/acs.jced.5b00294.

16. Serafin, J., Baca, Martyna., Biegun, M., Mijowska, E., Kalenczuk, R.J., Sreńscek-Nazzar, J. & Michalkiewicz, B. (2019). Direct conversion of biomass to nanoporous activated biocarbons for high CO_2 adsorption and supercapacitor applications. *Appl. Surf. Sci.* 497. DOI: 10.1016/j.apsusc.2019.143722.

17. Kapica-Kozar, J., Pirog, E., Kusiak-Nejman, E., Wróbel, R.J., Gęsikiewicz-Puchalska, A., Morawski, A.W., Narkiewicz, U. & Michalkiewicz, B. (2017). Titanium dioxide modified with various amines used as sorbents of carbon dioxide. *New. J. Chem.* 41, 1549–1557. DOI: 10.1039/c6nj02808j.

18. Gęsikiewicz-Puchalska, A., Zgrzebnicki, M., Michalkiewicz, B., Narkiewicz, U., Morawski, A.W. & Wróbel, R.J. (2017). Improvement of CO_2 uptake of activated carbons by treatment with mineral acids. *Chem. Eng. J.* 309, 159–171. DOI: 10.1016/j.cej.2016.10.005.

19. Sreńscek-Nazzal, J., Narkiewicz, U., Morawski, A.W., Wróbel, R., Gęsikiewicz-Puchalska, A. & Michalkiewicz, B. (2016). Modification of Commercial Activated Carbons for CO_2 Adsorption. *Acta Phys. Pol. A* 129, 394-401. DOI: 10.12693/APhysPolA.129.394.

20. Li, J., Michalkiewicz, B., Min, J., Ma, C., Chen, X., Gong, J., Mijowska, E. & Tang, T. (2019). Selective preparation of biomass-derived porous carbon with controllable pore sizes toward highly efficient CO_2 capture. *Chem. Eng. J.* 360, 250–259. DOI: 10.1016/j.cej.2018.11.204.

21. Kukulka, W., Cendrowski, K., Michalkiewicz, B. & Mijowska, E. (2019). MOF-5 derived carbon as material for CO_2 adsorption. *RSC Adv.* 9, 34349–34349. DOI: 10.1039/c9ra90077b.

22. Shi, X., Gong, J., Kierzek, K., Michalkiewicz, B., Zhang, S., Chu, P.K., Chen, X., Tang, T. & Mijowska, E. (2019). Multifunctional nitrogen-doped nanoporous carbons derived from metal-organic frameworks for efficient CO_2 storage and high-performance lithium-ion batteries. *New. J. Chem.* 43, 10405–10412. DOI: 10.1039/c9nj01542f.

23. Zgrzebnicki, M., Michalczyszyn, E. & Wrobel, R.J. (2018). Improving the Carbon Dioxide Uptake Efficiency of activated Carbons Using a Secondary Activation With Potassium Hydroxide, *Pol. J. Chem. Technol.*, 20(3), 87–94. DOI: 10.2478/pjct-2018-0043.

24. Michalkiewicz, B., Sreńscek-Nazzal, J. & Ziebro, J. (2009). Optimization of Synthesis Gas Formation in Methane Reforming with Carbon Dioxide. *Catal. Lett.* 129, 142–148. DOI: 10.1007/s10562-008-9797-6.

25. Michalkiewicz, B. (2006). The kinetics of homogeneous catalytic methane oxidation. *Appl. Catal. A* 307, 270–274. DOI: 10.1016/j.apcata.2006.04.006.

26. Michalkiewicz, B. (2003). Methane conversion to methanol in condensed phase. *Kinet. Catal.* 44, 801–805. DOI: 10.1023/B:KICA.0000009057.79026.0b.

27. Markowska, A. & Michalkiewicz, B. (2009). Biosynthesis of methanol from methane by Methylosinus trichosporium OB3b. *Chem. Pap.* 63, 105–110. DOI: 10.2478/s11696-008-0100-5.

28. Michalkiewicz, B. (2008). Assessment of the possibility of the methane to methanol transformation. *Pol. J. Chem. Technol.* 10, 20–26. DOI: 10.2478/v10026-008-0023-5.

29. Michalkiewicz, B., Sreńscek-Nazzal, J., Tabero, P., Grzmil, B. & Narkiewicz, U. (2008). Selective methane oxidation to formaldehyde using polymorphic T-, M-, and H-forms of niobium(V) oxide as catalysts. *Chem. Pap.* 62, 106–113. DOI: 10.2478/s11696-007-0086-4.

30. Michalkiewicz, B. (2004). Partial oxidation of methane to formaldehyde and methanol using molecular oxygen over Fe-ZSM-5. *Appl. Catal. A* 277, 147–153. DOI: 10.1016/j.apcata.2004.09.005.

31. Michalkiewicz, B. (2003). Partial oxidation of methane to oxygenates. *Przem. Chem*. 82, 627–628.

32. Michalkiewicz, B., Kalucki, K. & Sosnicki, J.G. (2003). Catalytic system containing metallic palladium in the process of methane partial oxidation. *J. Catal.* 215, 14–19. DOI: 10.1016/S0021-9517(02)00088-X.

33. Michalkiewicz, B., Jarosinska, M. & Lukasiewicz, I. (2009). Kinetic study on catalytic methane esterification in oleum catalyzed by iodine. *Chem. Eng. J.* 154, 156–161. DOI: 10.1016/j.cej.2009.03.046.

34. Jarosinska, M., Lubkowski, K., Sosnicki, J.G. & Michalkiewicz, B. (2008). Application of Halogens as Catalysts of CH(4) Esterification. *Catal. Lett.* 126, 407–412. DOI: 10.1007/s10562-008-9645-8.

35. Michalkiewicz, B. (2011). Methane oxidation to methyl bisulfate in oleum at ambient pressure in the presence of iodine as a catalyst. *Appl. Catal. A.* 394, 266–268. DOI: 10.1016/j.apcata.2011.01.014.

36. Majewska, J. & Michalkiewicz, B. (2016). Production of hydrogen and carbon nanomaterials from methane using Co/ZSM-5 catalyst. *Int. J. Hydrog. Energy* 41, 8668–8678. DOI: 10.1016/j.ijhydene.2016.01.097.

37. Majewska, J. & Michalkiewicz, B. (2014). Carbon nanomaterials produced by the catalytic decomposition of methane over Ni/ZSM-5 Significance of Ni content and temperature. *New Carbon Mater.* 29, 102–108. DOI: 10.1016/S1872-5805(14)60129-3.

38. Ziebro, J., Łukasiewicz, I., Grzmil, B., Borowiak-Palen, E. & Michalkiewicz, B. (2009). Synthesis of nickel nanocapsules and carbon nanotubes via methane CVD. *J. Alloys Compd.* 485, 695–700. DOI: 10.1016/j.jallcom.2009.06.039.

39. Ziebro, J., Lukasiewicz, I., Borowiak-Palen, E. & Michalkiewicz, B. (2010). Low temperature growth of carbon nanotubes from methane catalytic decomposition over nickel supported on a zeolite. *Nanotechnology* 21. DOI: 10.1088/0957-4484/21/14/145308.

40. Michalkiewicz, B. & Majewska, J. (2014). Diameter-controlled carbon nanotubes and hydrogen production. *Int. J. Hydrog. Energy* 39, 4691–4697. DOI: 10.1016/j.ijhydene.2013.10.149.

41. Sreńscek-Nazzal, J., Kamińska, Weronika., Michalkiewicz, B. & Koren, Z.C. (2013). Production, characterization and methane storage potential of KOH-activated carbon from sugarcane molasses. *Ind. Crops Prod.* 47, 153–159. DOI: 10.1016/j.indcrop.2013.03.004.

42. Keller, N., Ducamp, M., Robert, D., Keller, V. (2013) Ethylene Removal and Fresh Product Storage: A Challenge at the Frontiers of Chemistry. Toward an Approach by Photocatalytic Oxidation, Chem. Rev. 113(7), 5029–5070. DOI: 10.1021/cr900398v.

43. Wenelska, K., Michalkiewicz, B., Chen, X. & Mijowska, E. (2014). Pd nanoparticles with tunable diameter deposited on carbon nanotubes with enhanced hydrogen storage capacity. *Energy* 75, 549–554. DOI: 10.1016/j.energy.2014.08.016.

44. Wenelska, K., Michalkiewicz, B., Gong, Jiang., Tang, T., Kaleńczuk, R., Chen, X. & Mijowska, E. (2013). In situ deposition of Pd nanoparticles with controllable diameters in hollow carbon spheres for hydrogen storage. *Int. J. Hydrog. Energy* 38, 16179–16184. DOI: 10.1016/j.ijhydene.2013.10.008.

45. Baca, M., Cendrowski, K., Banach, P., Michalkiewicz, B., Mijowska, E., Kaleńczuk, R.J. & Zielińska, B. (2017). Effect of Pd loading on hydrogen storage properties of disordered

mesoporous hollow carbon spheres. *Int. J. Hydrog. Energy* 42, 30461–30469. DOI: 10.1016/j.ijhydene.2017.10.146.

46. Kukulka, W., Cendrowski, K., Michalkiewicz, B. & Mijowska, E. (2019). MOF-5 derived carbon as material for CO_2 absorption. *RSC Adv.* 9, 18527–18537. DOI: 10.1039/c9ra01786k.

47. Gong, J., Michalkiewicz, B., Chen, X., Mijowska, E., Liu, J., Jiang, Z., Wen, Xin. & Tang, T. (2014). Sustainable Conversion of Mixed Plastics into Porous Carbon Nanosheets with High Performances in Uptake of Carbon Dioxide and Storage of Hydrogen. *ACS Sustain. Chem. Eng.* 2, 2837–2844. DOI: 10.1021/sc500603h.

48. Zielińska, B., Michalkiewicz, B., Chen, X., Mijowska, E. & Kaleńczuk, R.J. (2016). Pd supported ordered mesoporous hollow carbon spheres. (OMHCS) for hydrogen storage. *Chem. Phys. Lett.* 647, 14–19. DOI: 10.1016/j.cplett.2016.01.036.

49. Baca, M.., Cendrowski, K., Kukulka, W., Bazarko, G., Moszynski, D., Michalkiewicz, B., Kalenczuk, R.J. & Zielińska, B. (2018). A Comparison of Hydrogen Storage in Pt, Pd and Pt/Pd Alloys Loaded Disordered Mesoporous Hollow Carbon Spheres. *Nanomaterials* 8. DOI: 10.3390/nano8090639.

50. Zielińska, B., Michalkiewicz, B., Mijowska, E. & Kalenczuk, R.J. (2015). Advances in Pd Nanoparticle Size Decoration of Mesoporous Carbon Spheres for Energy Application. Nanoscale Research Letters 10. DOI: 10.1186/s11671-015-1113-y.

51. Młodzik, J., Wróblewska, A., Makuch, E., Wróbel, R.J. & Michalkiewicz, B. (2016). Fe/EuroPh catalysts for limonene oxidation to 1,2-epoxylimonene, its diol, carveol, carvone and perillyl alcohol. *Catal. Today* 268, 111–120. DOI: 10.1016/j.cattod.2015.11.010.

52. Glonek, K., Wróblewska, A., Makuch, E., Ulejczyk, B., Krawczyk, K., Wróbel, Rafal. J., Koren, Z.C. & Michalkiewicz, B. (2017). Oxidation of limonene using activated carbon modified in dielectric barrier discharge plasma. *Appl. Surf. Sci.* 420, 873–881. DOI: 10.1016/j.apsusc.2017.05.136.

53. Lubkowski, K., Arabczyk, W., Grzmil, B., Michalkiewicz, B. & Pattek-Janczyk, A. (2007). Passivation and oxidation of an ammonia iron catalyst. *Appl. Catal. A,* 329, 137–147. DOI: 10.1016/j.apcata.2007.07.006.

54. Wróblewska, A., Makuch, E., Młodzik, J. & Michalkiewicz, B. (2017). Fe-carbon nanoreactors obtained from molasses as efficient catalysts for limonene oxidation. *Green Process. Synth.* 6, 397–401. DOI: 10.1515/gps-2016-0148.

56. Wróblewska, A., Makuch, E., Młodzik, J., Koren, Z.C. & Michalkiewicz, B. (2017). Fe/Nanoporous Carbon Catalysts Obtained from Molasses for the Limonene Oxidation Process. *Catal. Lett.* 147, 150–160. DOI: 10.1007/s10562-016-1910-7.

57. Wróblewska, A., Serafin, J., Gawarecka, A., Miadlicki, P., Urbas, K., Koren, Z.C., Llorca, J. & Michalkiewicz, B. (2020). Carbonaceous catalysts from orange pulp for limonene oxidation. *Carbon Letters* 30, 189–198. DOI: 10.1007/s42823-019-00084-2.

58. Wróblewska, A., Makuch, E., Młodzik, J., Koren, Z.C. & Michalkiewicz, B. (2018). Oxidation of limonene over molybdenum dioxide-containing nanoporous carbon catalysts as a simple effective method for the utilization of waste orange peels. *React. Kinet. Mech. Catal.* 125, 843–858. DOI: 10.1007/s11144-018-1468-z.

59. Kwiatkowski, M., Sreńscek-Nazzal, J. & Michalkiewicz, B. (2017). An analysis of the effect of the additional activation process on the formation of the porous structure and pore size distribution of the commercial activated carbon WG-12. *Adsorption* 23, 551–61. DOI: 10.1007/s10450-017-9867-4.

60. Kielbasa, K., Maciejewska, N., Kaminska, A. & Sreńscek-Nazzal, J. (2020). Porous carbon materials obtained from molasses carbon spheres. *Przem. Chem.* 99(11), 1636–1639. DOI: 10.15199/62.2020.11.9.

61. Zhao, X., Hirogaki, K., Tabata, I., Okubayashi, S. & Hori. T. (2006). A new method of producing conductive aramid fibers using supercritical carbon dioxide. Surf. Coat. Technol. 201(3–4) 628–636. DOI: 10.1016/j.surfcoat.2005.12.021.

62. Prasad,V.V. & Talupula, S. (2018). A Review on Reiforcement of Basalt and Aramid (Kevlar 129) fibers. *Mater. Today* 5(2), 5993–5998. DOI: 10.1016/j.matpr.2017.12.202.

63. Sutanu, S. & Singh, T.J. (2015). Characterisation of Kevlar Fiber and Its Composites: A Review. *Mater. Today* 2(4–5), 1381–1387. DOI: 10.1016/j.matpr.2015.07.057.

64. Qin, J., Guo, B., Zhang, L., Wang, T., Zhang, G. & Shi, X. (2020). Soft armor materials constructed with Kevlar fabric and a novel shear thickening fluid. *Compos. B. Eng.* 183, 107686. DOI:10.1016/j.compositesb.2019.107686.

65. Venkataraman, M., Xiong, X., Novotna, J., Kasparova, M., Mishra, R. & Militky, J. (2019) Thermal Protective Properties of Aerogel-coated Kevlar Woven Fabrics, *J. Fib. Bioeng. Inform.*12, 93–101. DOI:10.3993/jfbim00321.

66. Balaji, R., Nadarajana, M., Selokara, A., Kumara, S. & Sivakumar S. (2019). Modelling and analysis of Disk Brake under Tribological behaviour of Al-Al_2O_3 Ceramic Matrix Composites/Kevlar® 119 composite/C/Sic-Carbon Matrix Composite/Cr-Ni-Mo-V steel. *Mater. Today* 18, 3415–3427.

67. https://www.dupont.com/brands/kevlar.html ; access time 2021.06.08.

68. Castro-Muniz, A., Martınez-Alonso, A. & Tascon, J.M.D. (2008). Microporosity and mesoporosity of PPTA-derived carbons. Effect of PPTA thermal pretreatment, *Microporous and Mesoporous Mater.* 114, 185–192. DOI: 10.1016/j.micromeso.2008.01.003.

69. Conte, G., Stelitano, S., Policicchio, A., Minuto, F.D., Lazzaroli, V., Galiano, F. & Agostino, R.G. (2020). Assessment of activated carbon fibers from commercial Kevlar® as nanostructured material for gas storage: Effect of activation procedure and adsorption of CO_2 and CH_4. *J. Anal. Appl. Pyrolysis* 152, 104974. DOI:10.1016/j.jaap.2020.104974.

70. Zhang, Z., Yang, S., Zhang, P., Zhang, J., Chen, G. & Feng, X. (2019). Mechanically strong MXene/Kevlar nanofiber composite membranes as high-performance nanofluidic osmotic power generators. *Nat. Commun.* 10, 2920. DOI:10.1038/s41467-019-10885-8.

71. Suarez-Garcia, F., Martinez-Alonso, A. & Tascon, J.M.D. (2004). Nomex polyaramid as a precursor activated carbon fibers by phosphoric acid activation. Temperature and time effects. *Microporous Mesoporous Mater.* 75(1–2), 73–80. DOI: 10.1016/j.micromeso.2004.07.004.

72. Castro-Muniz, A., Martinez-Alonso, A. & Tascon, J.M.D. (2009). Effect of PPTA pre-impregnation with phosphoric acid on the porous materials texture of carbons materials prepared by CO_2 activation of PPTA chars. *Microporous Mesoporous Mater.* 119(1–3), 284–289. DOI: 10.1016/j.micromeso.2008.10.025.

73. Choma, J., Osuchowski, Ł., Marszewski, M., Dziura, A. & Jaroniec, M. (2016). Developing microporosity in Kevlar1-derived carbon fibers by CO_2 activation for CO_2 adsorption. *J. CO_2 Util.* 16, 17-22. DOI: 10.1016/j.jcou.2016.05.004 2212-9820.

74. Villar-Rodil, S., Navarrete, R., Denoyel, R., Albiniak, A., Paredes, J.I, Martinez-Alonso, A. & Tascon, J.M.D. (2005). Carbon molecular sieve cloths prepared by chemical vapour deposition of methane for separation of gas mixtures. *Microporous Mesoporous Mater.* 77(2–3), 109–118. DOI: 10.1016/j.micromeso.2004.08.017.

75. Villar-Rodil, S., Denoyel, R., Rouquerol, J. Martinez-Alonso, A. & Tascon, J.M.D. (2002). Characterization of aramid based activated carbon fibres by adsorption and immersion techniques. *Carbon*. 40(8), 1376–1380. DOI: 10.1016/S0008-6223(02)00114-8.